Fracture 1977, Volume 1, ICF4, Waterloo, Canada, June 19 - 24, 1977

WORKABILITY IN BULK FORMING PROCESSES

H. A. Kuhn* and G. E. Dieter**

ABSTRACT

An experimental fracture criterion based on the locus of the principal tensile and compressive strains at fracture is presented for bulk cold working processes. Limited data and examination of fracture mechanisms at high temperature suggest that the fracture criterion would be equally valid under hot working conditions. This fracture criterion line has been shown to be consistent with ductile fracture models based on localized thinning, void coalescence, and maximum tensile deformation energy. The fracture criterion line serves as a definitive and reproducible indicator of the basic ductility of the material. When the fracture line is combined with knowledge of the critical strain path in the workpiece as a function of the process parameters (such as die design, workpiece geometry, lubrication), workability can be evaluated simply and completely. An example of this approach is given for the cold heading of a bar.

DEFINITION OF WORKABILITY

Plastic working processes such as rolling, forging, and extrusion are designed to produce a useful semi-finished or finished shape, while at the same time changing or controlling the metallurgical structure to achieve a desired set of properties. Such operations are designated bulk forming processes since they involve a shape change through large changes in thickness dimensions and are distinguished from sheetforming processes, in which shape change is accompanied by relatively small changes in the thickness dimension. Workability, or formability, is a problem of major significance in both classes of processes, but the present paper deals only with workability in bulk forming processes.

Workability is defined as the degree of deformation that can be achieved in a particular metalworking process without fracture. That workability is not a function of material alone is pointed out by a comparison of the large cross-sectional area reduction obtainable with a single die in extrusion with the much smaller reduction possible under similar conditions in wiredrawing. The nominal compressive nature of stresses in extrusion delay the development of fracture while the tensile stresses in wiredrawing accelerate the fracture process. In general, workability depends on the local conditions of stress, strain, strain rate, and temperature in combination with material characteristics such as size, shape and distribution of second-phase particles. Moreover, the stress and strain state in a material undergoing a working process is not uniform, but varies from point to point.

* Howard A. Kuhn is Associate Professor of Metallurgical and Materials Engineering at the University of Pittsburgh

** George E. Dieter is Professor of Engineering at Carnegie-Mellon University Pittsburgh, Pa. U.S.A.

The stress and strain distributions, in turn, are determined by process parameters associated with die design, workpiece geometry, and lubrication. Control of these parameters can be used to produce conditions favorable for enhanced deformation before fracture.

These concepts have been expressed [1,2] by the relationship

$$\text{workability} = f_1 \text{ (material)} \times f_2 \text{ (process)} \qquad (1)$$

In this relationship, f_1 is a function of the basic ductility of the material and f_2 is a function of the stress system imposed by the process, largely defined by the secondary tensile stresses generated during the process. Thus, a workability analysis would include: (i) a fracture criterion (f_1) expressing the stress and/or strain states at fracture as a function of strain rate and temperature; and (ii) a description of the local stress, strain, strain rate, and temperature histories (f_2) at potential fracture sites in the material during the working process. The workability analysis is completed by comparing the local conditions existing in the material with the limiting conditions as expressed by the fracture criterion and then specifying the process variables which assure that the limiting conditions are not exceeded.

The present paper deals primarily with the development of fracture criteria (f_1) for bulk forming processes. Workability test techniques and experimentally determined fracture criteria are presented. The latter are then compared with predictions of various fracture modes.

Metalworking processes usually are carried out at strain rates between 1 and 500 s^{-1}. Hot working occurs at temperatures above 0.6 of the absolute temperature of the melting point (T_m), while cold working is conducted most often around 0.1 to 0.2 T_m. Most studies of fracture in metalworking have centered on cold working processes and a coherent picture of workability in such processes is developed in the subsequent sections of this paper. While the amount of fundamental studies of fracture in hot working is very limited, this knowledge is reviewed and shown to present a logical extension of the fracture criteria developed for cold working.

WORKABILITY TESTS

Development of experimental fracture criteria requires workability tests capable of providing a wide range of controlled stress and strain states. Tension, torsion, and upset compression tests are most widely used for this purpose. An important feature of each of these tests is the well-defined states of stress and strain.

Tension test

Uniform elongation during the tension test represents the best described and controlled mechanical property test [3]. The onset of necking, however, limits the amount of useful deformation that can be achieved in the test. In cold working, the strain at necking in the tension test generally is less than that achieved in most deformation processes. This limitation is even more serious in hot working, where greater deformation strains are achieved during processing, yet the strain to necking in tension is less than that in cold working.

The chief use of the tension test in workability testing is to evaluate the ductility of a material as a function of temperature. This is most often used in the hot working region to determine the maximum and minimum hot working temperatures. To provide useful information, the tension test must be conducted at strain rates comparable to hot working processes, usually faster than 1 s^{-1}. Most often this is accomplished by modifying an impact tester to break specimens in tension [4] or using a high-strain-rate tension testing machine. An increasingly popular high-rate tester is the Gleeble hot tensile test [5], which has the useful feature that the specimen is heated by self-resistance heating. Precise temperature control is possible and thermal cycles can be programmed to simulate a complete multipass thermomechanical history [6]. Experience with standardized specimens has shown [7] that hot workability is unacceptable when the reduction of area falls below 40 percent.

Because deformation becomes localized by necking very early in the hot tension test, it is not possible to conduct the test at even approximately constant strain rates. Since the strain rate variation is of the same order as those produced in the workpiece of industrial-scale metalworking systems, this limitation is of small consequence when the test is being used to establish the temperature limits for hot working. When fundamental data are to be collected at constant strain rate, the torsion test is preferred.

Torsion test

The torsion test subjects the material to a controlled ratio of shear to normal stress. High compressive normal stresses permit large shear strains without the limitation of a plastic instability. Moreover, because the strain rate is proportional to rpm, large values of constant shear strain rate are readily obtained [8]. Disadvantages of the torsion test are the radial gradient of stress and strain inherent in torsional deformation and the geometry, which may make it difficult to test specimens taken directly from an ingot. Axial stresses are developed when hot torsion specimens are deformed with fixed end constraint [9], which can result in unavoidable scatter in values of strain to fracture. The stress state in complex forming processes can be simulated by a combined stress torsion [10] test in which axial loads are superimposed on the torsional shear stresses.

Perhaps the greatest limitation of the torsion test in workability evaluation is the fact that the stress state inherent in the torsion of a bar is not representative of the critical stress states encountered in most bulk forming processes. In most situations, the geometric constraint of the process (imposed strain) and the critical stresses are coaxial. As a result, there is no reorientation of the material planes of weakness (fiber structure) relative to the critical stresses. However, in the torsion test, the imposed rotational strain creates a fiber orientation that is very markedly changed relative to the imposed stress state. Moreover, this large rotational strain can create a very pronounced fiber structure in a material which originally had no anisotropy. Therefore, although the torsion test is well suited for evaluating the flow stress of metals as a function of strain, strain rate, and temperature, it has inherent limitations which restrict its use for basic fracture studies.

Upset test

Axial compression of cylinders provides a deformation test in which the average stress state is inherently similar to that of bulk deformation processes and necking instabilities are eliminated. The test may be used in a manner similar to tension testing to determine hot working temperature limits under deformation rates similar to those in actual processes [11].

The occurrence of barrelling of the cylindrical surface, once deemed a disadvantage, actually furnishes considerable flexibility to the test. Alteration of the die contact friction conditions and cylinder aspect ratio (height-to-diameter ratio) lead to variations of the barrel severity and, consequently, to variations in the secondary tensile hoop stress developed at the bulge surface [12,13]. Thus, the upset test can be utilized to provide a broad range of stress and strain states in the localized ragion of the equator of the bulge surface and may be used for experimental determination of fracture criteria.

For use as a refined workability test, upset test specimens are provided with small grid markings at the mid-height of the cylindrical surface, Figure 1. These markings may be applied by an electrochemical etching method, scribed lines, or indentation marks. Measurements of the grid displacements during various stages of the test permit calculation of the principal strain and stress histories. Strains are calculated from the logarithmic representation:

$$\varepsilon_z = -\ln(h_o/h), \quad \varepsilon_\theta = \ln(w/w_o) \tag{2}$$

where

h_o, h = initial and deformed vertical grid spacings, respectively

w_o, w = initial and deformed circumferential grid spacings, respectively.

Examples of strain histories and their variation with test conditions are given in Figure 2. When the die surfaces are frictionless, there is no barrelling and the circumferential strain increases at exactly half the rate of the axial strain, $\varepsilon_\theta = -\varepsilon_z/2$.

Stresses are calculated from the strain histories with the aid of the Levy-Mises equations

$$\sigma_\theta = (\alpha - 1/2)[(2\bar{\sigma}/\sqrt{3})/(1-\alpha+\alpha^2)^{1/2}]$$
$$\sigma_z = (\alpha/2 - 1)[(2\bar{\sigma}/\sqrt{3})/(1-\alpha+\alpha^2)^{1/2}] \tag{3}$$

where

$\alpha = -d\varepsilon_\theta/d\varepsilon_z$, the rate of increase of circumferential strain with axial strain

$\bar{\sigma}$ = equivalent stress and is a function of total equivalent strain, $\bar{\varepsilon}$, where $\bar{\varepsilon} = \int d\bar{\varepsilon} = (1/\sqrt{3}) \int (1-\alpha+\alpha^2)^{1/2}\, d\varepsilon_\theta$

Figure 3 illustrates the stress histories associated with the strain histories of Figure 2. Note that for frictionless compression ($\varepsilon_\theta = -\varepsilon_z/2$), $\alpha = 1/2$, and $\sigma_\theta = 0$. Then for larger values of α, which result from greater barrelling due to frictional constraint, the circumferential stress σ_θ takes on increasingly tensile values. In addition, when α becomes

greater than 2, the axial stress at the barrelled surface also becomes tensile.

Although the results given in Figures 2 and 3 are from cold deformation tests, similar techniques can be utilized in hot deformation. Equations (2) and (3) are equally valid for hot deformation. Measurement of local surface strains is somewhat more difficult in hot deformation, and the technique must be modified. Materials with working temperatures below ~500°C can be monitored through electrochemically-etched grids, while those having a higher working temperature require indentation marks of sufficient depth to avoid loss by scale break-off. In either case, the test must be performed by compressing a series of identical specimens in sequence to progressively larger reductions until fracture occurs. The sequence of specimens then provides the strain history and the strain at fracture.

It is recognized that chilling of the specimen at the die surfaces will occur in hot upset tests. Since the material flow stress is higher where chilling occurs, this will have an effect on the stress distribution at the mid-height location of the specimen. Thus, care should be taken to insure that approximately the same degree of temperature gradient occurs in laboratory upset tests as in the actual process which is being modelled. For upset tests carried out in a mechanical press at rates in excess of 30 s^{-1} the die chilling effect is negligible.

EXPERIMENTAL FRACTURE CRITERION

The upset test is well suited for establishing experimental fracture criteria for bulk forming processes since it undergoes a deformation mode similar to bulk forming processes. Moreover, the test may be conducted with a variety of controlled stress and strain states. Through the grid measurements and strain and stress calculations, Equations (2) and (3), a variety of stress and/or strain criteria may be evaluated.

The characterization of test results that provides the simplest description and is most readily applied to processes is the locus of principal surface strains at fracture. An example is given in Figure 4 for cold deformation of 1045 steel [13]. The tensile circumferential strain and compressive axial strain are plotted on the coordinate axes. For each test, the data fit a straight line with a slope of negative one-half. Decreasing friction at the die-workpiece interface increases the strains at fracture. Within a given friction condition, each point represents a different specimen with aspect ratio varying from 0.5 to 1.75.

Similar straight-line relationships have been determined for other ferrous and non-ferrous materials under cold upsetting deformation [14,15]. An evaluation of fracture strain measurements in upsetting by other investigators shows similar straight-line relationships [12,16,17]. In each case, the slope of the straight line is one-half and the intercept with the tensile strain axis changes in accordance with the inherent ductility of the material.

The similarity of the fractures strain relationships observed by Kuhn, et al. [13] and several other investigators [12,15,17] implies that the straight-line relationship between principal compressive and tensile surface strains at fracture is a characteristic result of the ductile fracture process, and that the line can be treated as a fracture criterion representing the workability of the material. If the upset tests for determi-

nation of the fracture line are carried out at the same strain-rate and temperature as used in the actual process under study, then the fracture line serves as the material function (f_1) in the workability relationship given in Equation (1).

The upset test technique for experimental determination of a fracture criterion has been extended to sintered powder materials. Results for two aluminum alloy powders [18] are shown in Figure 5. Both alloys have the same fracture line for cold deformation, and the intercept in this case is considerably lower than those of fully-dense materials [12-17]. More importantly, upset tests on the same materials at a hot working temperature of 700°F (370°C) also show the straight-line behavior observed for room temperature deformation. Figure 6 gives additional results for fracture during hot working of a sintered low-alloy steel powder [18]. The straight line plot of fracture strains suggest that the total strain fracture criterion is valid for hot working as well as cold working and for sintered powder metals, as well as fully-dense metals.

Application of the forming limit concept embodied in the fracture lines described previously requires an understanding of the relationships between local principal surface strains in the potential fracture regions of the deformation process of interest. This can be accomplished through detailed plasticity analysis of the process, e.g., in references [19,20], or through experimental analysis [18,21] using model materials and the grid techniques described previously for upset tests. The strain relationships in the potential fracture regions can be altered by changing process parameters such as die design, workpiece geometry, and lubrication. Such parameters constitute the process function (f_2) in the workability relationship, Equation (1). Workability analysis involves changing the process parameters so that the deformation strain relationships (f_2) do not exceed the fracture strain line for the material at the appropriate strain rate and temperature (f_1). An example of application of this forming limit concept to preform design for powder forging is given in reference [22].

A schematic illustration of workability analysis is given in Figure 7. In the bolt heading process shown, if it is required to form a bolt head of diameter D on a rod of diameter d, the required circumferential strain is ln(D/d). Suppose strain path a describes the relationship between the local strains at the bulging surface of the head for a particular friction condition. Consider, further, that the material to be utilized has the forming limit line labelled A. In order for the bolt head to be formed fully, the strain path a must cross the fracture limit A, and cracking is likely. One approach to avoid defects is to use a material having a higher fracture strain line, such as B. Another approach is to alter the strain path to b so that the full head diameter is reached before the strain path crosses fracture line A. In this example, improving lubrication is the only modification available for altering the strain path. In more complex cases, however, die design and workpiece geometry changes will also be effective in altering the strain path.

FRACTURE MODELS

A qualitative picture of the ductile fracture mechanism has become clear through a careful series of studies [23-25] which have been summarized in review articles [26,27]. It is evident that ductile fracture consists of three successive events: (i) voids form at points where compatibility of plastic deformation is difficult, such as grain boundary triple-points,

inclusions, and second-phase particles, even for deformation that is macroscopically uniform; (ii) the voids enlarge and elongate along planes of maximum shear; (iii) finally, the voids coalesce and fracture is complete. It is clear that inhomogeneous localized deformation is an integral part of the ductile fracture process, and that tensile stress plays a strong role in accentuating the effects of this deformation. The quantitative influence of each of these factors is not completely understood. Various mathematical models of ductile fracture have been presented in an attempt to provide this understanding. Three such models are reviewed below, and reformulated for comparison with the experimentally determined fracture criterion described previously.

Localized thinning model

In sheetforming, the observation that a neck forms prior to fracture, even under biaxial stress conditions in which localized instability cannot occur, has prompted consideration of the effects of inhomogeneities in the material. A model of localized thinning due to a small inhomogeneity has been devised by Marciniak and Kuczynski [28]. Beginning with the model depicted in Figure 8, plasticity mechanics is applied to determine the rate of thinning of the constricted region relative to that of the thicker surrounding material. When the rate of thinning reaches a critical value, the limiting strains are considered to have been reached, and a forming limit diagram can be constructed. The analysis includes the effects of crystallographic anisotropy, workhardening rate, and inhomogeneity size.

This model was applied to free surface fractures in bulk forming processes by Lee and Kuhn [14], because of evidence that localized instability and thinning precedes this type of ductile fracture [29]. Two model geometries were considered, one having a groove in the axial direction (Z-model), and the other having a groove in the radial direction (R-model), Figure 8. Applying plasticity mechanics to each model, it is considered that fracture has occurred when the thin region has reduced to zero thickness. When these fracture strains are plotted for different applied stress ratios, a fracture strain line can be constructed. As shown in Figure 9, the predicted fracture line matches the essential features of the experimental fracture lines. The slope is -1/2 over most of the strain range. However, prediction of the height of the fracture line depends strongly on the assumed initial value of the groove thickness. At the present time, this is the subject of considerable speculation. Despite this shortcoming, the model shows that for an applied strain ratio $d\varepsilon_\Theta/d\varepsilon_Z = -1/2$ (frictionless compression), the tensile stress is zero and no fracture is predicted. That is, even when an inhomogeneity exists, unless there is a tensile stress, the inhomogeneity remains dormant and does not grow to form a fracture.

Void growth models

Microscopic observations of void growth and coalescence along planes of maximum shear leading to fracture led McClintock [30] to develop a model of hole growth. Again, plasticity mechanics is applied to the analysis of deformation of holes within a shear band. When the elongated holes come into contact, it is considered that fracture has occurred. When the McClintock model is evaluated for a range of applied stress combinations, a fracture strain-line can be constructed.

Figure 10 gives an example of calculated results from the McClintock model in comparison with the experimental fracture line. Again, the predicted fracture strain line has a shope of -1/2, matching that of the experimental fracture line. Therefore, as in the case of the inhomogeneity model, Figure 9, an applied strain ratio of -1/2 (tensile stress equal to zero) does not lead to fracture. Thus, even though holes exist in the material, coalescence into a fracture does not occur unless a finite tensile stress is present. Also, as in the case of the inhomogeneity model, the height of the predicted fracture line is strongly dependent on the initial inhomogeneity strength (ratio of hole diameter to spacing) and is difficult to determine in real materials.

Cockcroft model

The Cockcroft criterion of fracture is not based on a micromechanical model of fracture, but simply recognizes the roles of tensile stress and plastic deformation [31]. It is suggested that fracture occurs when the tensile strain energy reaches a critical value

$$\int_0^{\bar{\varepsilon}_f} \sigma^* d\bar{\varepsilon} = C \qquad (4)$$

where σ^* = maximum tensile stress
$\bar{\varepsilon}$ = equivalent strain
C = constant for given material, temperature, and strain rate; determined by experiment.

The criterion was successfully applied by Cockcroft and Latham to cold working processes. The criterion was also reformulated by Kuhn et al. [13] to provide a predicted fracture line for comparison with the experimental fracture strain line. Figure 11 shows that the fracture strain line predicted by the Cockcroft criterion, Equation (4), also is in reasonable agreement with the experimental results. Height of the predicted fracture line is determined by experiment, such as a tension test, rather than by speculation on a material inhomogeneity strength.

Sellars and Tegart [32] also have applied the Cockcroft criterion to hot working processes. Reasonable agreement was obtained in comparison of fracture strains in hot torsion and tension of aluminum, nickel, and copper over temperature ranges of $0.5<T/T_m<0.8$ and strain rates of 1 sec^{-1} and 8 sec^{-1}.

All three fracture models considered in this section predict accurately the slope characteristic of the experimental fracture criterion. Void coalescence and localized thinning are apparently described accurately by the micromechanical models, but the weakness of these models is their inability to predict the height of the fracture line. One possible improvement would be consideration of the problem of void initiation around second phase particles, since each of the models assumes the preexistence of voids. The role of tensile stress is also clear; without a finite tensile stress, voids or inhomogeneities remain dormant and do not grow to produce fracture.

EXTENSION OF FRACTURE CRITERION TO HOT WORKING

Fracture models based on localized thinning, void coalescence, and maximum tensile deformation energy accurately predict the slope characteristic of the fracture criterion. This implies that the role of tensile stress in determining the rate of localized thinning or hole growth is modelled accurately. Although much of the work done on the fracture criterion described in this paper has been carried out on cold working processes, there is considerable evidence that the same fracture line criterion is valid for hot working. Figures 3 and 4 give fracture lines with characterestic slope of one-half for the hot working of sintered compacts of aluminum alloy and low alloy steel powder. In addition, Sellers and Tegart [32] reported successful correlations for fracture in hot deformation using the Cockcroft criterion, which in turn has been shown to provide an accurate description of the experimental fracture criterion line, Figure 11.

The general relationship between fracture mode and temperature and strain-rate is shown in Figure 12, based on work by Wray [33]. For strain rates in excess of about 1 sec^{-1}, ductile fracture predominates. At less than about 0.6 T_m a void coalescence mode of ductile fracture would be expected. The hot working mechanisms that are operative at $T>0.6\ T_m$ have been studied extensively in recent years [34]. For low stacking fault metals, e.g., nickel, copper, iron, softening occurs by dynamic recrystallization, while high stacking fault metals, e.g., aluminum and austenitic iron, soften by dynamic recovery in which a stable well-developed subgrain structure is formed. High temperature deformation introduces the new factor that grain boundary sliding can be important, especially at lower strain rates. Thus, an important new mechanism of void initiation by grain boundary sliding at particles in grain boundaries or atomistic scale grain boundary ledges is introduced by high temperature. However, under hot working conditions, crack propagation becomes the major factor controlling ductility, rather than void initiation. Figure 13, taken from torsion tests on an austenitic iron-nickel-chromium alloy [10] shows that the strain to propagate a crack increases into the hot working region ($T > 1400^{\circ}F$) and becomes the major component of the total strain to fracture. Crack propagation is by a link-up of voids. When voids initiated on the original grain boundaries have difficulty in linking up because boundary migration is high as a result of dynamic recrystallization, the hot ductility is high. In extreme cases, this can lead to the highly ductile rupture illustrated schematically in Figure 12. The similarity between crack propagation by void linkup and the void sheet mechanism for ductile fracture at lower temperatures have been recognized by Fleck, Beevers, and Taplin [35]. This provides a theoretical basis for expecting the fracture line criterion to be valid for true hot working as well as cold working, since the ductile fracture mechanisms, although different in fine detail, are similar.

With strain rates below about 1 s^{-1}, the easy nucleation of voids by grain boundary sliding and the reduced rate of dynamic softening can lead to extensive internal cavity formation. An extensive literature on cavitation as it affects creep ductility has been developed [36], but it is not directly relevant to fracture in hot working. However, depending upon the location of the boundaries between fracture modes in Figure 12, there may be a low ductility region at an intermediate working temperature [37,10]. This occurs when the temperature and strain rate are too low to bring about rapid recrystallization. Under these conditions, grain boundary initiated voids lead to rapid intergranular fracture with low ductility. Since the fracture mechanism differs appreciably from void sheet coalescence or void linkup, it is not expected that the fracture line criterion would apply.

It is more likely that in this strain-rate/temperature region the fracture criterion would be given by a Griffith-Orowan type of relationship in which continuous crack propagation occurs when a crack reaches a critical length for a given applied stress [38,35].

CONCLUSIONS

The linear fracture strain locus can be considered as a general macroscopic criterion of surface fracture in bulk forming processes. The line may be determined readily for a given material, temperature, and strain rate from upset tests on cylindrical specimens. Combining this description of the fracture characteristics of the material with a description of the surface strain relationships leads to a method of analysis of workability problems in bulk forming processes.

The characteristic slope of the fracture criterion line has been shown to be consistent with ductile fracture models based on localized thinning, void coalescence, and maximum tensile deformation energy. Limited experimental data and consideration of the modes of high-temperature fracture suggest that the fracture criterion line will be valid at hot working conditions.

REFERENCES

1. LATHAM, D.J. and COCKCROFT, M.J., Nat. Eng. Lab., Report No. 216, 1966.
2. GITTINS, A., J. Australian Inst. Metals 20, 1975, 184.
3. DIETER, G.E., Mechanical Metallurgy, 2nd Edition, Chapter 9, McGraw-Hill Book Company, 1976.
4. GITTINS, A., SELLARS, C.M. AND NORTHWAY, L.G., J. Materials 7, 1972, 155.
5. NIPPES, E., et al, Weld J., 1955, 1832.
6. WEISS, B., et al, Weld J., 35, 1970, 471s.
7. BAILEY, R.E., Met. Eng. Quart., 1975, 43.
8. ROBIN, J.L., et al, J. Materials, 2, 1967, 271.
9. MOROZUMI, F., Iron Steel Inst. Japan, 8, 1968, 14.
10. SHAPIRO, E. and DIETER, G.E., Met. Trans., 1, 1970, 1711.
11. SABROFF, A.M., BOULGER, F.W. and HENNING, A.J., Forging Materials and Practices, Reinhold, 1968, 120.
12. KOBAYASHI, S., Trans. ASME, J. Eng. Ind. 92B, 1970, 391.
13. KUHN, H.A., LEE, P.W. and ERTURK, T., Trans. ASME, J. Eng. Mat. and Tech., 95H, 1973, 213.
14. LEE, P.W. and KUHN, H.A., Met. Trans., 4, 1973, 969.
15. SHAH, D.C., Mechanical Working and Steel Processing, XII, TMS-AIME New York, 1974.
16. KUDO, H. and AOI, K., J. Jap. Soc. Tech. Plasticity, 8, 1967, 17.
17. THOMASON, P.F., Int. J. Mech. Sci., 11, 1969, 187-198.
18. KUHN, H.A., SUH, S.K. and ROBINSON, M.L., Progress in Powder Metallurgy A75, 31, MPIF, 159.
19. LEE, C.H. and KOBAYASHI, S., Proc. North American Metalworking Research Conference, 1, 1973, 159.
20. SUH, S.K., KUHN, H.A. and DOWNEY, C.L., "Metal Flow and Fracture in an Extrusion-Forging Process", accepted for publication in Trans. ASME, J. Eng. Mat. and Tech.
21. KUHN, H.A. and SUH, S.K., Proc. Third North American Metalworking Research Conference, Carnegie Press, 1975, 262.

22. DOWNEY, C.L. and KUHN, H.A., Trans. ASME, J. Eng. Mat. and Tech., 97H, 1975, 121.
23. PUTTICK, K.E., Phil. Mag., 4, 1959, 964.
24. ROGERS, JR., H.C., Trans. AIME, 218, 1960, 498.
25. BLUHM, J.E. and MORRISSEY, R.J., Proc. 1st Int. Conference on Fracture, 3, Chapter DII, Sendai, Japan, 1965, 93.
26. ROGERS, JR., H.C., Ductility, ASM, 1967, 31.
27. ROSENFIELD, A.R., Met. Rev., 121, 1968, 29.
28. MARCINIAK, Z. and KUCZYNSKI, K., Int. J. Mech. Sci., 9, 1967, 609.
29. KUHN, H.A. and LEE, P.W., Met. Trans., 2, 1971, 3197.
30. McCLINTOCK, F.A., Trans. ASME, J. Appl. Mech., 90, 1968, 363.
31. COCKCROFT, M.G. and LATHAM, D.J., Inst. Metals, 96, 1968, 33.
32. SELLARS, C.M. and TAGART, W.J. McG., Int. Met. Rev., 17, 1972, 1.
33. WRAY, P.J., J. Appl. Physics, 40, 1969, 4018.
34. JONAS, J.J., SELLARS, C.M. and TAGERT, W.J. McG., Met. Rev., 14 (130), 1969, 1.
35. FLECK, R.G., BEEVERS, C.J. and TAPLIN, D.M.R., Met. Sci., 9, 1975.
36. PERRY, A.J., J. Mat. Sci., 9, 1974, 1016.
37. RHINES, F.N. and WRAY, P.J., Trans. ASM, 54, 1961, 117.
38. TAPLIN, D.M.R., J. Australian Inst. Metals, 10, 1965, 336.

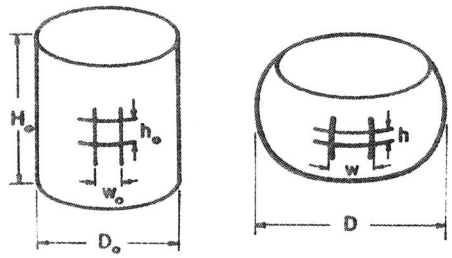

AXIAL STRAIN $\varepsilon_z = \ln(h/h_o)$
HOOP STRAIN $\varepsilon_\theta = \ln(w/w_o)$ or $\ln(D/D_o)$

Figure 1 Diagram of the upset test specimen illustrating grid marks for strain measurements on the bulge surface

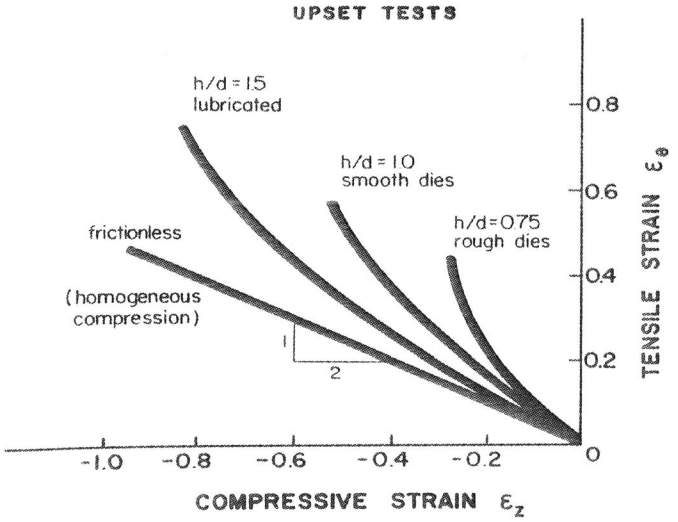

Figure 2 Relationship between surface strains during upsetting, illustrating the effects of friction and specimen aspect ratio (h/d)

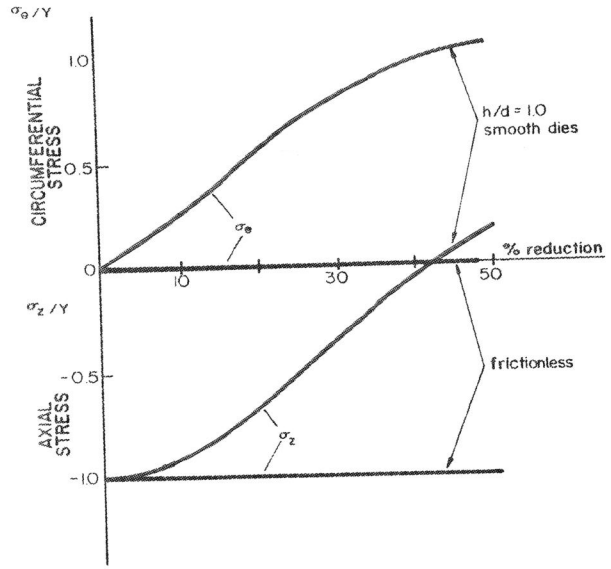

Figure 3 Stresses calculated from the strain paths in Figure 2 with the aid of Equation (2)

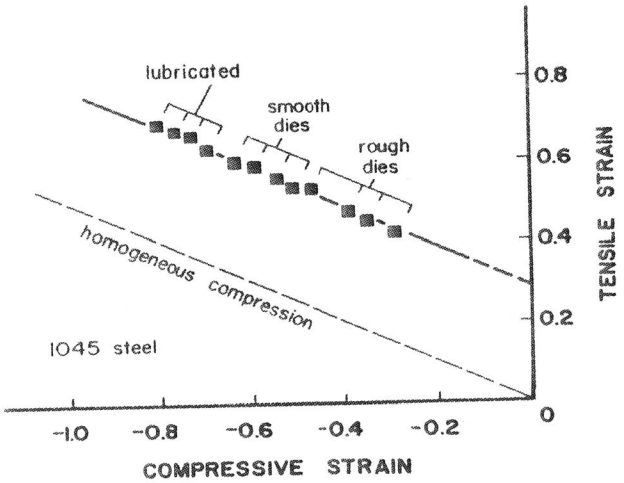

Figure 4 Locus of surface strains at fracture in upset tests on 1045 steel at room temperature

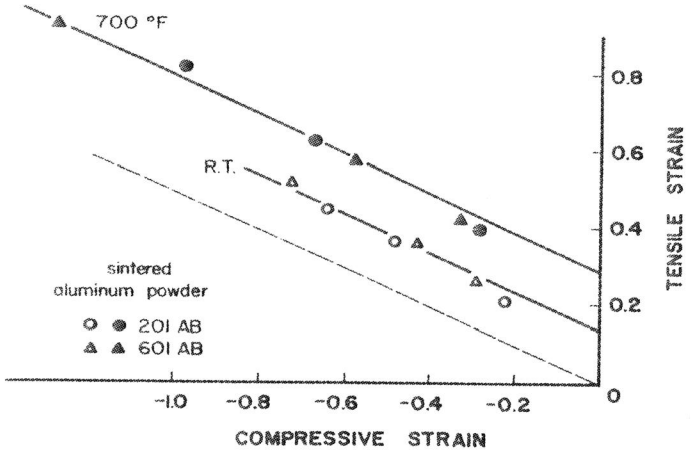

Figure 5 Locus of surface strains at fracture in upset tests on 201 AB and 601 AB aluminum alloy powders a room temperature and at 700°F (370°C)

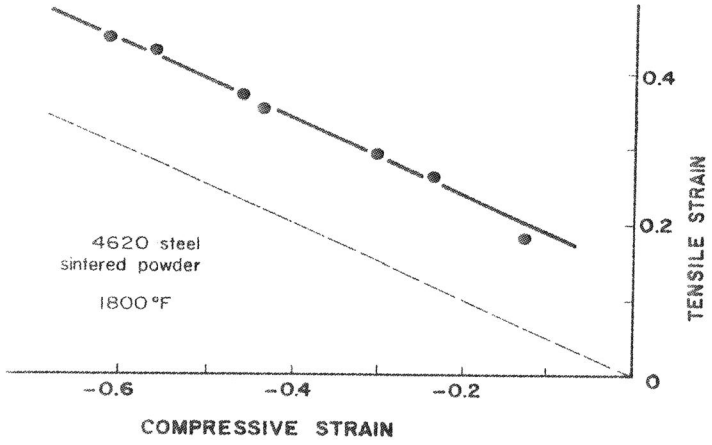

Figure 6 Locus of surface strains at fracture in upset tests on 4620 steel powder at 1800°F (980°C)

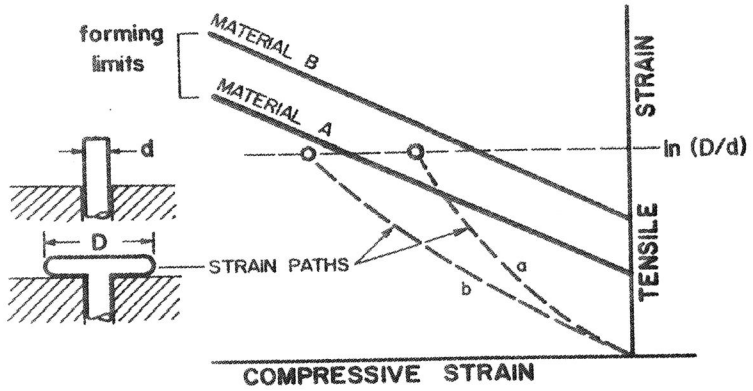

Figure 7 Schematic illustration of the interaction of strain paths (f_2) and material formability lines (f_1) in bolt heading operations

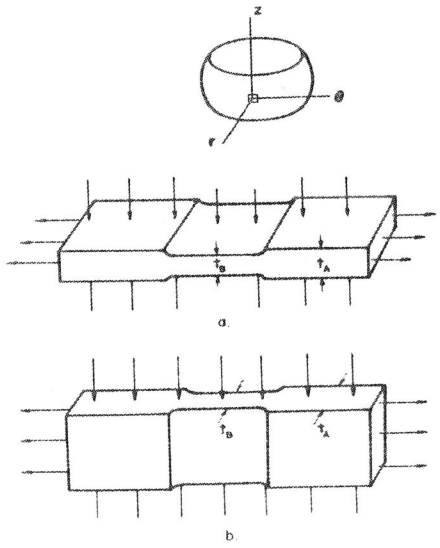

Figure 8 Models for analysis of localized thinning and fracture in sheetforming [28] and the surface of upset cylinders [14]

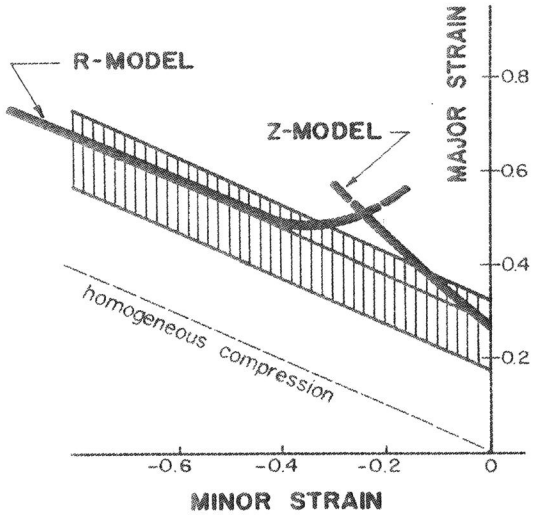

Figure 9 Fracture strain locus predicted by the model of localized thinning. The shaded region represents the range of fracture lines determined experimentally.

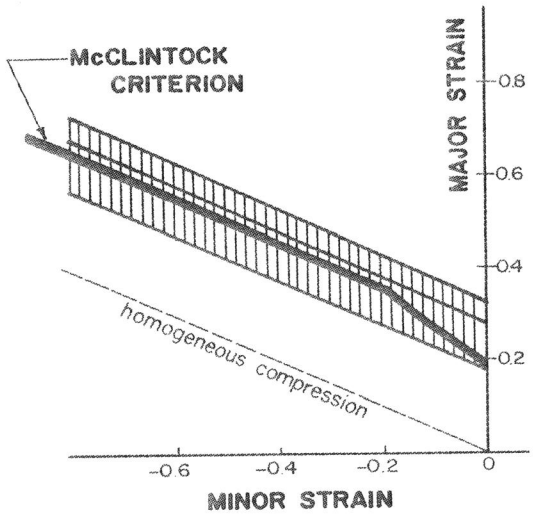

Figure 10 Fracture strain locus predicted by the McClintock model of void growth. The shaded region represents the range of fracture lines determined experimentally

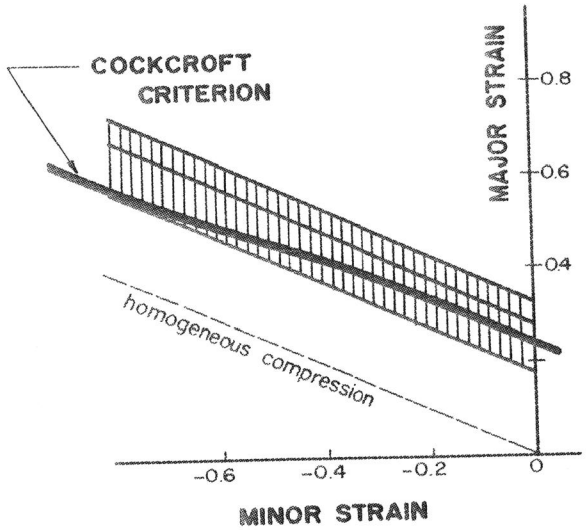

Figure 11 Fracture strain locus predicted by the Crockcroft criterion. The shaded region represents the range of fracture lines determined experimentally

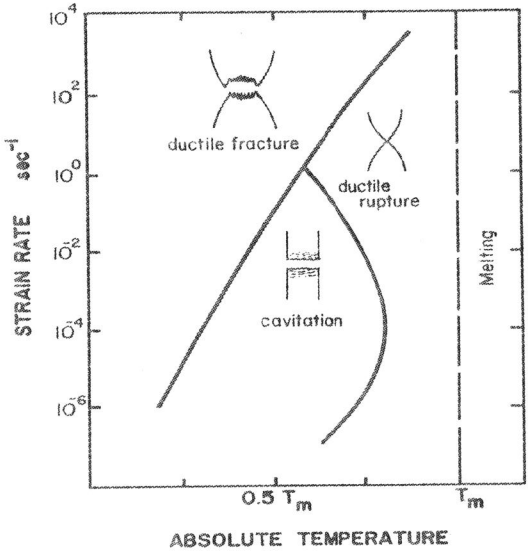

Figure 12 Schematic illustration of tensile fracture modes in strain rate-temperature space. (After Wray [33])

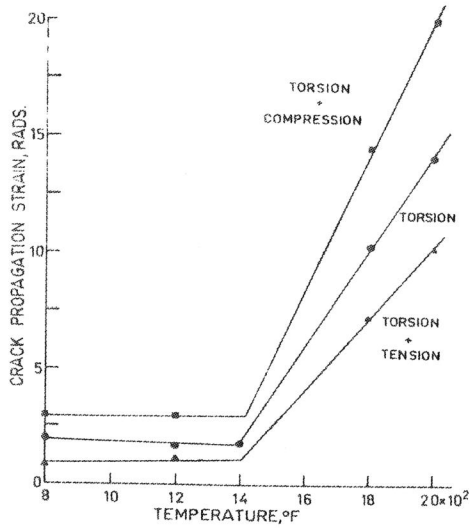

Figure 13 Crack propagation strain as a function of temperature in combined stress torsion tests on Inconel 600 [10]